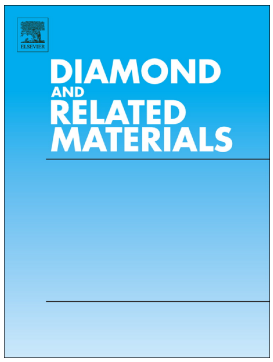

Comparison of HPHT and LPHT annealing of Ib synthetic diamond

N.M. Kazuchits, M.S. Rusetsky, V.N. Kazuchits, O.V. Korolik, V. Kumar, K.S. Moe, W. Wang, A.M. Zaitsev

PII: S0925-9635(18)30471-0
DOI: https://doi.org/10.1016/j.diamond.2018.11.018
Reference: DIAMAT 7262

To appear in: *Diamond & Related Materials*

Received date: 4 July 2018
Revised date: 16 November 2018
Accepted date: 21 November 2018

Please cite this article as: N.M. Kazuchits, M.S. Rusetsky, V.N. Kazuchits, O.V. Korolik, V. Kumar, K.S. Moe, W. Wang, A.M. Zaitsev , Comparison of HPHT and LPHT annealing of Ib synthetic diamond. Diamat (2018), https://doi.org/10.1016/j.diamond.2018.11.018

Comparison of HPHT and LPHT annealing of Ib synthetic diamond

N. M. Kazuchits[a], M. S. Rusetsky[a], V. N. Kazuchits[a], O. V. Korolik[a], V. Kumar[b], K. S. Moe[d], W. Wang[d], A. M. Zaitsev[c,d,*]

[a)] Belarusian State University, Nezavisimosti ave. 4, 220030, Minsk, Belarus

[b)] Suffolk County Community College, Brentwood, NY 11784, USA

[c)] The College of Staten Island / CUNY, 2800 Victory Blvd., Staten Island, NY 10312, USA

[d)] Gemological Institute of America, 50 W 47th St #800, New York, NY 10036, USA

[*)] corresponding author: alexander.zaitsev@csi.cuny.edu

Abstract

Defect transformations in type Ib synthetic diamond annealed at a temperature of 1870 °C under stabilizing pressure (HPHT annealing) and in hydrogen atmosphere at normal pressure (LPHT annealing) are compared. Spectroscopic data obtained on the samples before and after annealing prove that the processes of nitrogen aggregation and formation of nitrogen-nickel complexes are similar in both cases. Essential differences between HPHT and LPHT annealing are stronger graphitization at macroscopic imperfections and enhanced lattice distortions around point defects in the latter case. The lattice distortion around point defects is revealed as a considerable broadening of zero-phonon lines of "soft" (vacancy-related) optical centers. It was found that LPHT annealing may enhance overall intensity of luminescence of HPHT-grown synthetic diamonds.

Keywords*: high pressure high temperature annealing, low pressure high temperature annealing, synthetic type Ib diamond, nitrogen aggregation, graphitization, spectral broadening.*

1. Introduction

High temperature annealing is a common method used for defect transformation in diamonds. Aggregation of nitrogen [1] and removal of radiation defects [2-4] are two most common examples. Since diamond at normal pressure is a metastable phase of carbon, it experiences spontaneous graphitization when exposed to high temperatures. The graphitization rate (diamond-to-graphite phase transition) increases exponentially with temperature. Temperatures below 1500 °C can be considered low temperatures, at which diamond can be kept in vacuum or inert atmosphere for very long time without noticeable bulk graphitization. Temperatures over 1700 °C are high temperatures. At these temperatures, graphitization can be very fast strongly depending on the pressure and environment in which diamond is heated, the crystallographic orientation of sample facets and crystal quality [5-7]. Our multiple experiments on high temperature annealing of diamond in vacuum and in various gasses show that at a temperature of 1800 °C in a vacuum of 10^{-5} mbar a perfect diamond plate oriented in (100) plane can stand several hours with only trace of graphite on its surface. In contrast, in low vacuum of

0.1 mbar, a few micron graphite layer forms in a few minutes on diamond surface oriented along (110) plane when heated at temperature 1800 °C. Crystal lattice defects, in particular macroscopic defects like inclusions and microcracks, stimulate graphitization considerably.

In order to reduce the graphitization rate, high temperature annealing is frequently performed at a pressure, which makes diamond more thermodynamically stable. A typical example of such an annealing is high pressure and high temperature (HPHT) treatment at temperatures 1800-2300 °C under pressure of 50 kbar [8]. HPHT treatment is a preferred technique of high temperature annealing of diamond in terms of minimum graphitization. However, its technical implementation is not simple. It takes bulky, costly high-pressure equipment and well-trained staff.

Elimination of technical problems of HPHT annealing is the driving force of development of methods of annealing of diamond at low pressure, high temperature (LPHT) in simple furnaces. In order to minimize graphitization during LPHT annealing the heating is performed either in high vacuum or in hydrogen. Although no systematic studies have been performed on LPHT annealing of diamond yet, our experiments reveal two important features of high temperature heating of diamond without stabilizing pressure. Firstly, the graphitization of perfect diamond crystal occurs always at its surface and never in the bulk. Any graphitization inside the diamond bulk is triggered by some internal imperfections, like inclusions, bundles of dislocations, or microcracks. Secondly, the atmosphere, in which heating is performed, is crucial for the surface graphitization rate. The chemical interaction of diamond surface with the atoms present in the surrounding gas may catalyze graphitization (oxygen) or inhibit it (hydrogen). So far, the best results in terms of minimum graphitization during LPHT annealing were achieved in pure hydrogen [9, 10].

HPHT and LPHT annealings are thermodynamically very different processes. An obvious question is whether the transformation of defects in diamond lattice, e.g. aggregation of nitrogen and formation of optically active point defects, occurs differently too. Comparison of the data from the available reports on HPHT and LPHT annealing [8, 11-20] suggests that there are some differences. However, since those annealings were performed in different regimes with different samples, it is speculative to suggest that the differences in the defect transformations are the effect of pressure. Below, we present results of direct comparison of defect transformations in identical samples of HPHT-grown synthetic diamond subjected to HPHT and LPHT annealings performed in identical temperature-time regime.

2. Samples preparation, annealing and measurements

Two yellow single crystal type Ib synthetic diamonds produced by AdamasInvest, Ltd [21], were used for this research. The diamonds were synthesized by temperature gradient method in C-Fe-Ni melt at temperature in the range 1350–1450 °C and pressure in the range 4.5–5.0 GPa for 60-70 hours. The metal growth medium composition was 70 wt% of iron and 30 wt% of nickel. Details of the growth procedure can be found in [22]. Of the variety of available as-grown diamonds several crystals with relatively large cubic growth sectors ({100} sectors) and octahedral growth sectors ({111} sectors) were selected. Two adjacent plates #2152-4 and #2152-5 were cut along plane (100) of the central part of one of the crystals. These two plates were the primary samples on which most of the data were obtained. Two (100)-oriented plates #5699-1 and #5699-2 were cut of another crystal close to its sides. The plates were mechanically polished to thickness varying from 0.32 mm to 0.8 mm. The plates #2152-4 and #5699-1 (one plate of each crystal) were annealed together at a temperature of 1870 °C at a pressure of 5.2 GPa in high pressure apparatus BARS [23] for 4 hours (HPHT annealing). The other two plates #2152-5 and #5699-2 were annealed in HTT-G10 graphite furnace [24] in hydrogen at the same temperature 1870 °C for 3.5 hours at an absolute pressure of 105 kPa (LPHT annealing). Details of LPHT annealing procedure

can be found in [10, 15, 25, 26]. After annealing, the graphitized surface layer was removed in oxygen plasma and/or by heating in air at a temperature of 850 °C for a few minutes. Finally, the samples were chemically cleaned in saturated solution of sulfuric acid and potassium dichromate. Images of the samples were taken after final etching and cleaning. Transformation of defects was studied using optical absorption in UV, visible and IR spectral ranges at room temperature [10, 25] and photoluminescence (PL) at liquid nitrogen temperature (LNT).

Absorption in UV-Vis spectral range was measured with Agilent Cary 300 UV-VIS spectrophotometer. Diameter of the light beam probe on the sample was about 0.6 mm. Absorption measurements in IR spectral range were performed in a spectral range 650-4000 cm^{-1}. Thermo Scientific Nicolet iS50 spectrometer equipped with liquid nitrogen-cooled MCT detector and purged with nitrogen and Bruker Vertex 70 spectrometer were used for collecting general spectra from individual growth sectors of the samples. A diaphragm of 1.1 mm in diameter placed directly on sample surface over the measured growth sectors in the locations shown in Fig. 1a, c, e, g was used. Since the size of growth sectors was in the range 1 to 2 mm, the measurements through the said diaphragm gave us an adequate information about nitrogen aggregation over the whole growth sectors. Thermo Scientific Nicolet iN10 FTIR Microscope equipped with motorized stage, liquid nitrogen-cooled MCT detector and 50×50 μm aperture was used for the measurements with focused light beam passing separately through cubic growth sectors, octahedral growth sectors and through octahedral growth sector near boundary between sectors (Fig. 1f, h).

Intensity of IR absorption was measured relative to the diamond lattice intrinsic absorption, which is equal 4.6±0.3 cm^{-1} at wavenumbers 2560 cm^{-1} and 2430 cm^{-1} and 12.8±0.3 cm^{-1} at wavenumbers 2170 cm^{-1} and 2030 cm^{-1} [27]. Absorption coefficients of the main nitrogen centers were evaluated via decomposition of the measured spectra in three components: absorption of C-defects (single substitutional nitrogen atoms in neutral charge state), absorption of N^+-defects (positively charged single substitutional nitrogen atoms) and absorption of A-defects (close pairs of substitutional nitrogen atoms). Concentrations of the corresponding defects were calculated using the relations from [28-30]. C-defect concentration relates to the absorption strength of the band at wavenumber 1130 cm^{-1} as N_C [ppm] = $25 \cdot \alpha_{1130}$ [cm^{-1}]. Concentration of A-defects can be found from the absorption strength of the band at wavenumber 1280 cm^{-1}: N_A [ppm] = $16.5 \cdot \alpha_{1280}$ [cm^{-1}]. Concentration of N^+-defects relates to the absorption intensity of the line at wavenumber 1332 cm^{-1} as N_{N+} [ppm] = $5.5 \cdot \alpha_{1332}$ [cm^{-1}]. The concentrations of C-, N^+- and A-defects presented in Table 1 were obtained from the general spectra taken from the whole growth sectors and from the spectra measured locally at the inter-sector boundary.

Photoluminescence (PL) measurements were performed using Renishaw inVia Raman confocal spectrometers with laser excitation at wavelengths 324.8 nm (He-Cd metal vapor laser), 457.0 nm (Ar-ion laser), 514.5 nm (Ar-ion laser) and 830.0 nm (diode laser). During the measurements, samples were kept immersed in liquid nitrogen. The measurement procedure was similar to that described in [31]. Spectral resolution of all PL measurements was 0.15 nm for lasers 324.8, 457.0 and 514.5 nm and 0.5 nm for laser 830.0 nm.

For comparison of PL intensities of optical centers measured in different samples and in different spots of one and the same sample, the intensities of spectra were adjusted to equal intensity of Raman line. Since the efficiency of Raman scattering at the center of Brillouin zone does not depend much on the presence of point defects up to relatively high defect concentration, intensity of 1332 cm^{-1} Raman line can be used as an internal measure of the emission intensity. Thus, the measurements of PL intensity relative to Raman line intensity allows a semi-quantitative comparison of PL efficiency for different intensities of excitation, different geometries of collection of the emitted light and for samples with different quality of surface. A justification of such an approach can be drawn from the data and analysis presented in [32].

Raman spectra were measured at room temperature using spectrometer Nanofinder High End (LOTIS TII Tokyo Instruments) combined with 3D scanning confocal microscope. Laser excitation was performed at wavelengths 355 nm and 473 nm (solid state lasers). Spectral resolution was about 0.25 cm^{-1}. Perfection of diamond crystal lattice was evaluated from the spectral width of Raman line.

3. Results and discussion

3.1. Visual examination

Two adjacent plates #2152-4 and #2152-5 cut from one crystal are shown in Fig. 1. The images (a, c, e, g) show the samples on white background under day light illumination. The images (b, d, f, h) were taken on black non-luminescent background under UV laser illumination at a wavelength of 337 nm (photoluminescence images). In the latter case, it is seen that the plates contain cubic growth sectors (labeled with "**c**") and octahedral growth sectors (labeled with "**o**"). The white dotted lines show the sector boundaries. Two other plates #5699-1 and #5699-2 cut from octahedral growth sectors of another crystal were about 2×2 mm^2 in size (not shown in Fig. 1).

Before annealing, the plates did not reveal any internal macroscopic defects when examined with optical microscope (except a crack precursor in cubic sector of sample #2152-5). The octahedral sectors were dark yellow whereas the cubic sectors had a bit lighter yellow color. It is known that the main cause of yellow color of type Ib synthetic diamonds is absorption of C-defects [33, 34]. Thus, we assume that the octahedral sectors contain a higher concentration of nitrogen than the cubic ones.

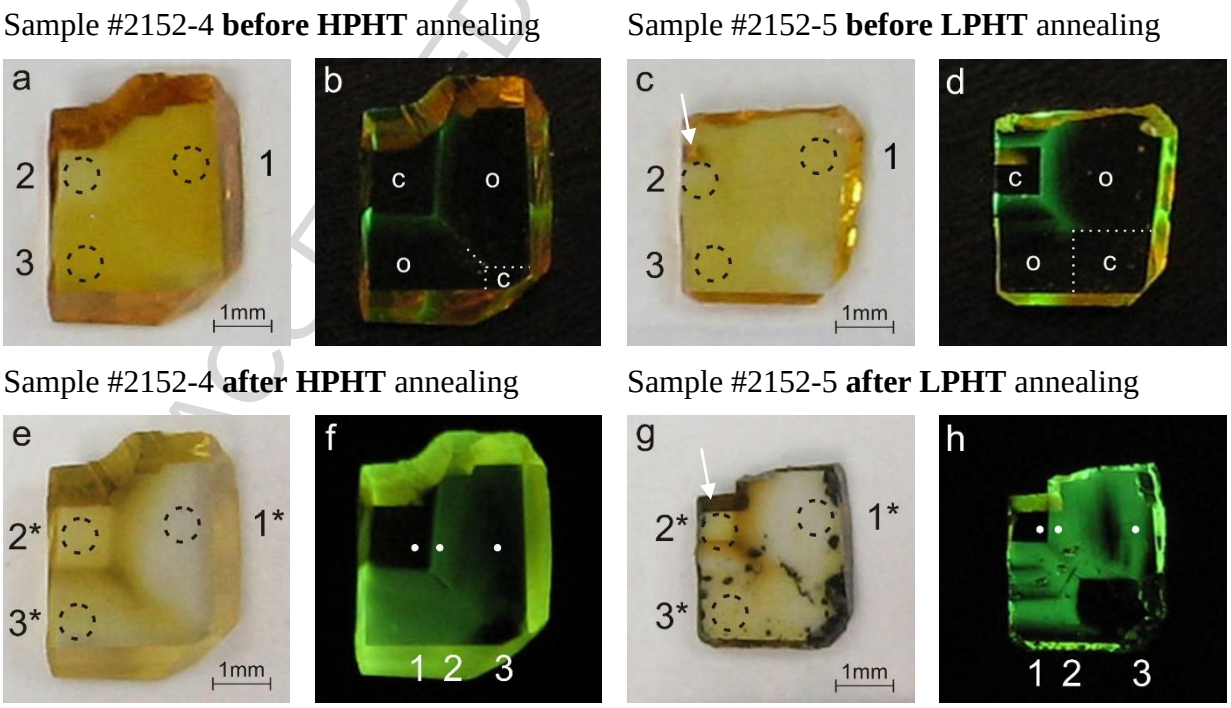

Fig. 1. Optical (a, c, e, g) and luminescence (b, d, f, h) images of samples before (a, b, c, d) and after HPHT (e, f) and LPHT (g, h) annealing (surface graphitization is removed). The boundaries between cubic and octahedral growth sectors are shown with white dotted lines on the PL images obtained before annealing. Dashed circles show areas of UV-Vis absorption measurements and IR

absorption measurements of general spectra of individual growth sectors. Sites of the measurements of focused IR absorption and PL are shown with white dots labeled 1 (cubic sector), 2 (octahedral sector near boundary between sectors) and 3 (octahedral sector). White arrow in images (c, g) marks the largest graphitized crack formed after LPHT annealing.

Under UV excitation, all samples reveal green luminescence surrounding cubic growth sectors. This luminescence is related to Ni-containing defects [35-39]. Starting from the inter-sector boundary, the luminescence intensity abruptly disappears in cubic growth sector, whereas it gradually reduces over octahedral sectors. This characteristic distribution of luminescence intensity evidences high efficiency of uptake of nickel impurity during growth at inter-sector boundaries and in octahedral sectors [38-39]. Sample #2152-5, which was cut close to the seed, captured more nickel and was exposed to high temperature for a longer time during crystal growth. Therefore, more luminescence-active Ni-containing defects were formed in it and the green luminescence in this sample covers larger area [36, 37].

After HPHT annealing, no major damage of samples occurred: surface of the samples was slightly etched, but no graphitization was seen. LPHT annealing was more destructive. In this case, a piece broke away from the sample because of graphitization of the crack shown with white arrow (Fig. 1g). The surface graphitization was minor on (100) surfaces whereas it was substantial on (111) surfaces.

After both HPHT and LPHT annealings color of cubic sectors remained almost unchanged. In contrast, color of octahedral sectors turned light-yellow or, in some areas, even almost colorless. In both annealing cases, the inter-sector boundaries turned yellow-brown. The distribution of color at the boundaries was very abrupt from the cubic sector side and diffused from the octahedral sector side. The green luminescence increased in intensity and spread all over the octahedral growth sectors. Distribution of intensity of the green luminescence remained non-homogeneous and it followed the distribution of nickel concentration [35-39]. In cubic growth sectors, the green luminescence was negligible suggesting low nickel concentration.

3.2. UV-Vis absorption

Visual changes in color were in agreement with the changes in absorption spectra taken in UV and visible spectral ranges (Fig. 2). Before annealing, absorption of both samples had an onset at a wavelength of 500 nm and gradual increase toward shorter wavelengths (absorption due to C-defects [40, 41]). This absorption was stronger in octahedral sectors (traces 1) and weaker in cubic sectors (traces 2). After annealing, absorption spectra of cubic sectors remained almost unchanged (traces 2*), whereas the onset in the spectra of octahedral sectors shifted considerably towards shorter wavelengths (traces 1* and 3*). After HPHT annealing, the absorption onset was at a wavelength of 320 nm. In case of LPHT annealing, the absorption increase started at a wavelength of 370 nm. In both cases, absorption in the visible spectral range in octahedral sectors became significantly lower.

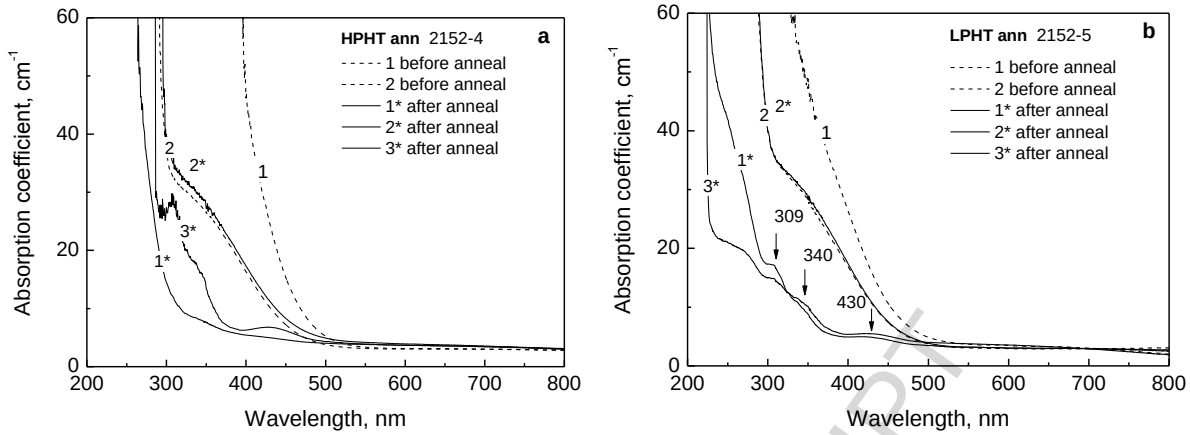

Fig. 2. Absorption spectra in UV-visible spectral range before (1 - octahedral growth sector; 2 - cubic growth sector) and after (1*, 3* - octahedral growth sectors; 2* - cubic growth sector), HPHT (a) and LPHT (b) annealing. The labels of the spectra correspond to the numbers of the areas marked with dashed circles in Fig 1.

The absorption spectra in octahedral sectors of the annealed samples resembled those of natural type IaA diamonds [40, 41] and suggested substantial aggregation of nitrogen in both annealing cases. In contrast, minor change in absorption spectra of cubic sectors was indicative of slow aggregation processes.

The spectra taken from the areas with strong green luminescence (trace 3* for HPHT, and traces 1* and 3* for LPHT) revealed broad absorption features at wavelengths 430 nm, 340 nm and 309 nm. All these absorptions are characteristic of nitrogen- and nickel-containing diamonds annealed at high temperatures [27, 42-46]. Remnants of these bands were the reason of the persisting yellow-brown color which cannot be completely eliminated by high temperature annealing. Multiple experiments performed previously on different samples showed that the differences in the absorption strength of the bands 309, 340 and 430 nm actually did not depend on the annealing method but on the presence of some defects. Since the nature of these defects is unknown, we do not discuss behavior of the bands 309, 340 and 430 nm in this communication.

3.3. IR absorption

IR absorption measured in cubic sectors, octahedral sectors and close to the boundary between sectors revealed transformation of diamond type from Ib in IaA in octahedral sectors. The results were similar to those published in [42, 46]. The concentrations of nitrogen C- and A-defects as well as the aggregation rate (A-defect concentration versus total nitrogen concentration) calculated from these spectra are presented in Table 1.

Before annealing, the octahedral growth sectors of both plates contained nitrogen predominantly in form of C-defects in concentration 145-150 ppm. Content of the aggregated nitrogen in form of A-defects was negligible amounting only 1% to 2%. After annealing, the dominating form of nitrogen was A-defect. The rate of aggregation varied from 70% to 100%. Same changes in IR absorption spectra of samples occurred for samples #5699-1 and #5699-2 too.

Absorption spectra measured in cubic sectors did not reveal noticeable changes after annealing in both cases (Fig. 3a, d). The aggregation was about 16% in cubic sector of the sample processed with HPHT annealing and about 6% in cubic sector of the sample processed with LPHT annealing.

The presence of aggregated nitrogen in as-grown samples was a manifestation of high temperature annealing, which HPHT-grown diamonds had experienced during their growth. The low rate of nitrogen aggregation in cubic sectors measured spectroscopically agreed with their remaining yellow color. Comparable aggregation rates for HPHT and LPHT annealings with very different aggregation rates in different sectors suggested that pressure was not a major factor in the processes of aggregation of C-defects into A-defects at temperatures up to 1900 °C, whereas the presence of nickel was decisive. The catalytic action of nickel for nitrogen aggregation in synthetic diamonds was discussed in [47]. Thus, the lower nitrogen aggregation rates in cubic sectors suggested lower concentration of nickel impurity captured into cubic sectors as compared with the octahedral ones.

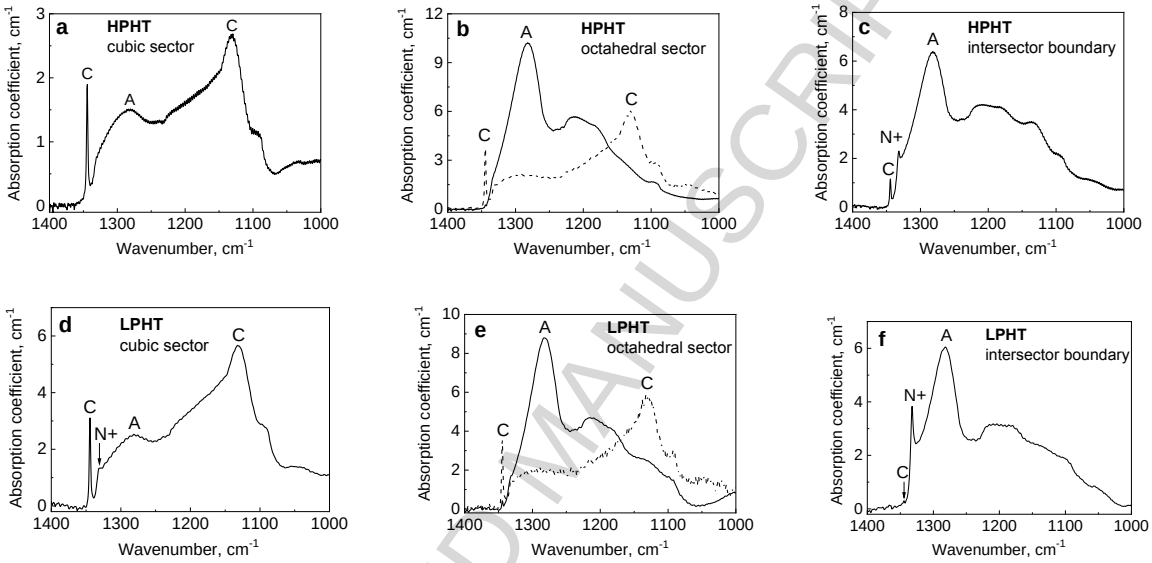

Fig. 3. Representative FTIR absorption spectra taken from equivalent points (shown in Fig. 1f, h) of cubic sectors (a, d), octahedral sectors (b, e) and close to inter-sector boundary (c, f) of HPHT annealed sample #2152-4 (upper row) and LPHT-annealed sample #2152-5 (lower row). Dashed traces in (b, e) show spectra of octahedral sectors measured before annealing. The initial spectra for cubic sectors (not shown) are identical to those shown in (a, d).

Table 1. Concentrations of nitrogen defects after annealing

Nitrogen concentration after HPHT anneal, ppm					Nitrogen concentration after LPHT anneal, ppm				
Sample, growth sector	C	N^+	A	A/total	Sample, growth sector	C	N^+	A	A/total
#2152-4, cubic {100}	60.0	0	11.6	16%	#2152-5, cubic {100}	127.5	1.1	8.3	6%
#2152-4, octahedral {111}	0	0	160.1	100%	#2152-5, octahedral {111}	20.0	0	140.3	88%

#2152-4, at boundary {100}/{111}	52.5	2.2	89.1	62%	#2152-5, at boundary {100}/{111}	22.5	8.3	89.1	74%
#5699-1, octahedral {111}	33.8	2.2	118.8	77%	#5699-2, octahedral {111}	55.0	0	136.3	71%

It is seen in Table 1 that in both annealing cases the nitrogen aggregation rate is less and the concentration of N^+ defects is greater at the inter-sector boundary than at the periphery of the octahedral sectors. Formation of N^+ defects in HPHT-grown synthetic diamond has been attributed to Ni impurities [39]. It has been also assumed that nitrogen, when in positive charge state, aggregates much more slowly. Thus, it appears that nickel plays two opposite roles in nitrogen aggregation: it can stimulate aggregation by changing charge state of nitrogen [48], or inhibit aggregation by, probably, forming stable nickel-nitrogen complexes. The coexistence of these two conflicting processes supports the assumption made in [10] that for the maximum nitrogen aggregation and removal of yellow color in HPHT-grown diamonds, the nitrogen and nickel impurities must be present in matching concentrations. If the content of nickel is too low or too high, the nitrogen aggregation during high temperature heating is only partial.

It is worth mentioning that IR absorption spectra have not revealed obvious presence of B-aggregates of nitrogen. Thus, the second stage of nitrogen aggregation, namely conversion of A-defects into B-defects, is negligible at temperatures below 1900 °C for both HPHT and LPHT annealing.

3.4. Photoluminescence and Raman

Before annealing, photoluminescence of cubic sectors was dominated by nickel-related center S2 with zero-phonon line (ZPL) at 489 nm. Minor H3 (ZPL at 503 nm), NV^0 (ZPL at 575 nm) and NV^- (ZPL at 637 nm) centers were detected too (Fig. 4a). In octahedral sectors excited with 514.5 nm laser, only very weak NV^- center was detected (Fig. 4d). After annealing, in cubic growth sectors, the luminescence was dominated by nitrogen-related centers, whereas in octahedral growth sector, nitrogen produced minor luminescence. The major luminescence of octahedral sectors was due to centers related to metals used as catalysts of diamond growth [44, 49]. In most cases they were Ni-related defects. Ni-related centers with ZPLs at 477 nm, 489 nm, 497 nm (S3 center), 523 nm, 727.4 nm, 793 nm were created in both cases of HPHT and LPHT annealing. Atomic structure of the defects responsible for this luminescence has not been established yet. However, it was assumed that some of them are complexes of nickel with A-aggregates of nitrogen [25, 35, 42, 50-53].

It is remarkable that luminescence of NV^- center could not be detected in octahedral sectors even with excitation with 514.5 nm laser, which is the most efficient for PL of NV^- center. Two reasons of the absence of NV^- emission were, firstly, the strong nickel-nitrogen interaction and conversion of most N-related defects into Ni-N complexes and, secondly, the action of Ni-related defects as acceptors. Low position of Fermi level in nickel-containing synthetic diamonds keep NV defects in positive or neutral charge state. Indeed, emission of NV^0 centers (neutral charge state of NV defects) was well present in PL spectra of octahedral sectors (Fig. 4d).

Multiple photoluminescence measurements in different points of LPHT-annealed and HPHT-annealed samples revealed that in general luminescence intensity was stronger after LPHT

annealing than after HPHT annealing. The stronger luminescence of LPHT-annealed samples was observed for most nitrogen-related and nickel-related optical centers through the whole visible and near IR spectral range for wavelengths from 400 nm to 1000 nm (Fig. 4). This effect was especially pronounced for luminescence excited with 514.5 nm laser. In this case PL intensity after LPHT annealing was at least an order of magnitude stronger than after HPHT annealing for both growth sectors (Fig. 4c).

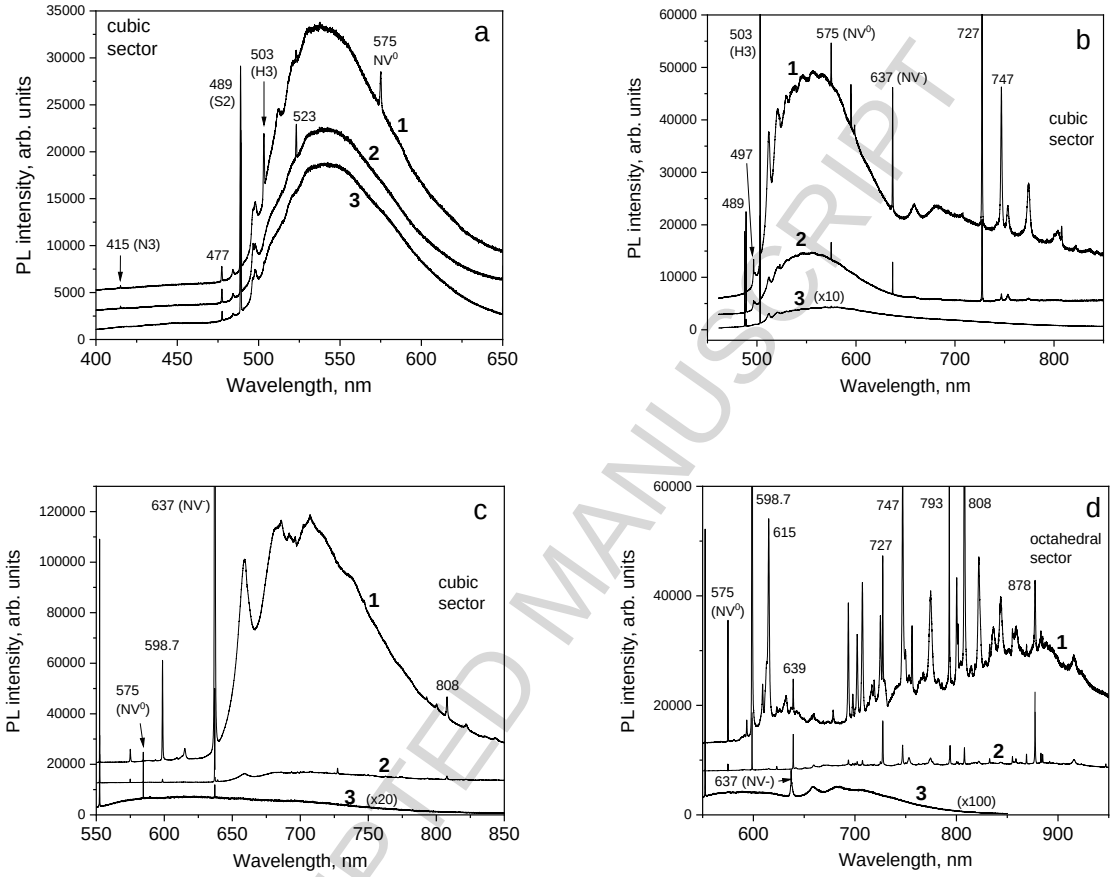

Fig. 4. Comparison of photoluminescence spectra excited with lasers at wavelength 324.8 nm (a), 457.0 nm (b) and 514.5 nm (c, d). Traces (1) - LPHT annealing, traces (2) - HPHT annealing, traces (3) - initial spectra before annealing. Intensities of spectra in each graph are adjusted to equal intensity of Raman line. The spectra (2) and (3) are shifted vertically for clarity. All spectra were measured at liquid nitrogen temperature. Note that intensity of initial spectrum is multiplied by 10 in (b), by 20 in (c) and by 100 in (d) for clarity.

Although the luminescence intensity of LPHT-annealed samples was stronger than that of HPHT-annealed ones, the set of optical centers was qualitatively the same in both cases. However, relative intensity of emission of some centers may differ considerably. Some minor centers formed after LPHT annealing may not be seen in spectra after HPHT annealing due to their low intensity (Fig. 5).

For now, we do not have any reasonable explanation of the enhanced luminescence intensity in LPHT-annealed synthetic diamond. Two possible mechanisms could be the increase in concentration of optical centers and the promotion of luminescence via suppression of non-

radiative channels (suppression of luminescence quenching). Though, for now, no evidence can be provided for either of these mechanisms.

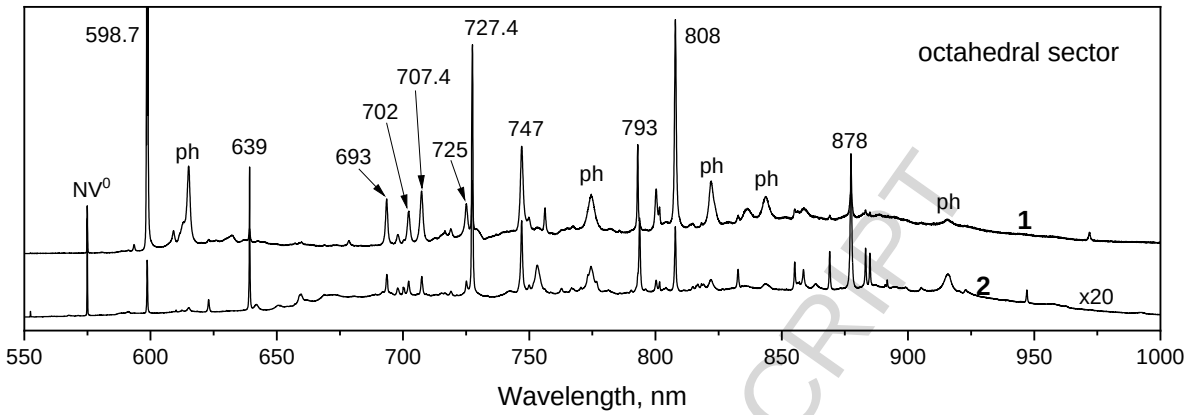

Fig. 5. Comparison of PL spectra taken from octahedral sectors of LPHT-annealed sample (1) and HPHT-annealed sample (2). Spectral position of major ZPLs is shown. Broad lines related to quasilocal vibrations are labeled with (ph). Intensity of spectrum (2) is increased 20 times for clarity.

Our previous studies of LPHT annealing of similar samples in hydrogen at a temperature of 1800 ºC for 20 hours revealed no formation of N3 centers [25]. After 3.5 hours annealing at temperature 1870 ºC we did observe traces of luminescence of N3 centers (Fig. 4a), which were indicators of formation of B-defects. Thus, we concluded that temperature was a critical parameter of formation of B-defects, which could be created in a measurable amount only at temperatures close to 1900 °C.

A remarkable difference between HPHT and LPHT annealings was much broader ZPLs of some optical centers in the latter case. This broadening was particularly strong for nitrogen-related centers H3, NV^-, NV^0, H2 and Ni-related centers 707.4 nm and 747 nm (Fig. 6a-f). Although the broadening might be quite large, the lines did not exhibit any significant spectral shift.

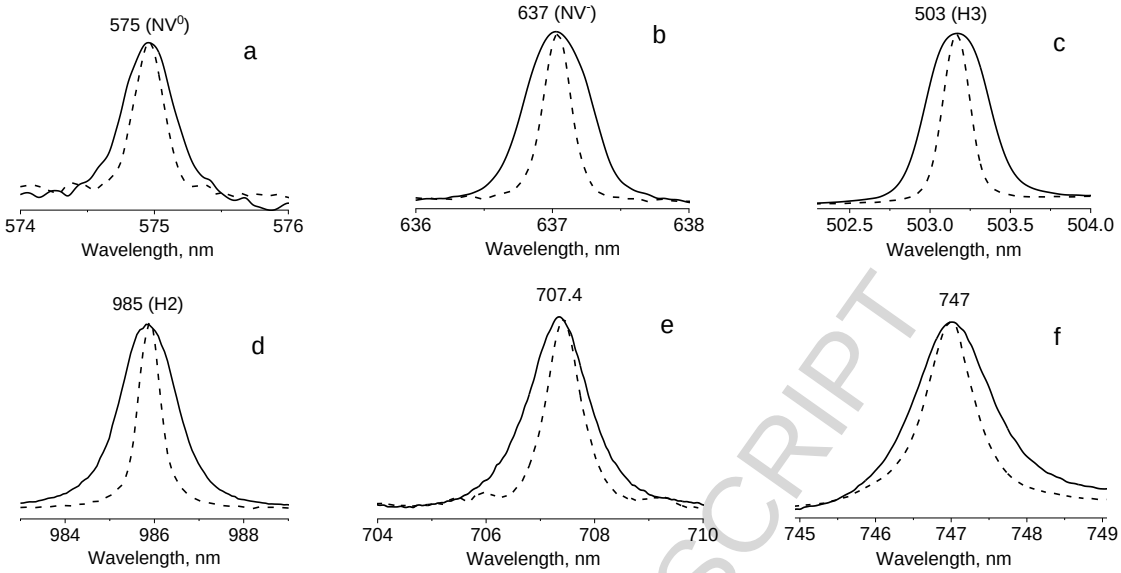

Fig. 6. Photoluminescence spectra of ZPLs of nitrogen-related centers NV^0 (a), NV^- (b), H3 (c), H2 (d), 707.4 nm (e) and 747 nm (f) measured in HPHT-annealed (dashed traces) and LPHT-annealed (solid traces) samples. Peak intensities of the lines are adjusted to equal magnitude for clarity. Spectra (a-d) were taken from cubic sectors, while spectra (e, f) were taken from octahedral sectors.

Most of Ni-related centers and nitrogen-related N3 center did not exhibit substantial broadening of their ZPLs after LPHT annealing. Some of these lines are shown in Fig. 7. In octahedral sectors, unfortunately, the nitrogen-related centers NV^-, H3 and H2 were not detected. Thus, we could not compare widths of their ZPLs in octahedral sectors. In contrast, luminescence of NV^0 center was strong in octahedral sectors under 514.5 nm laser excitation. The broadening of ZPL of NV^0 center in cubic and octahedral sectors was comparable.

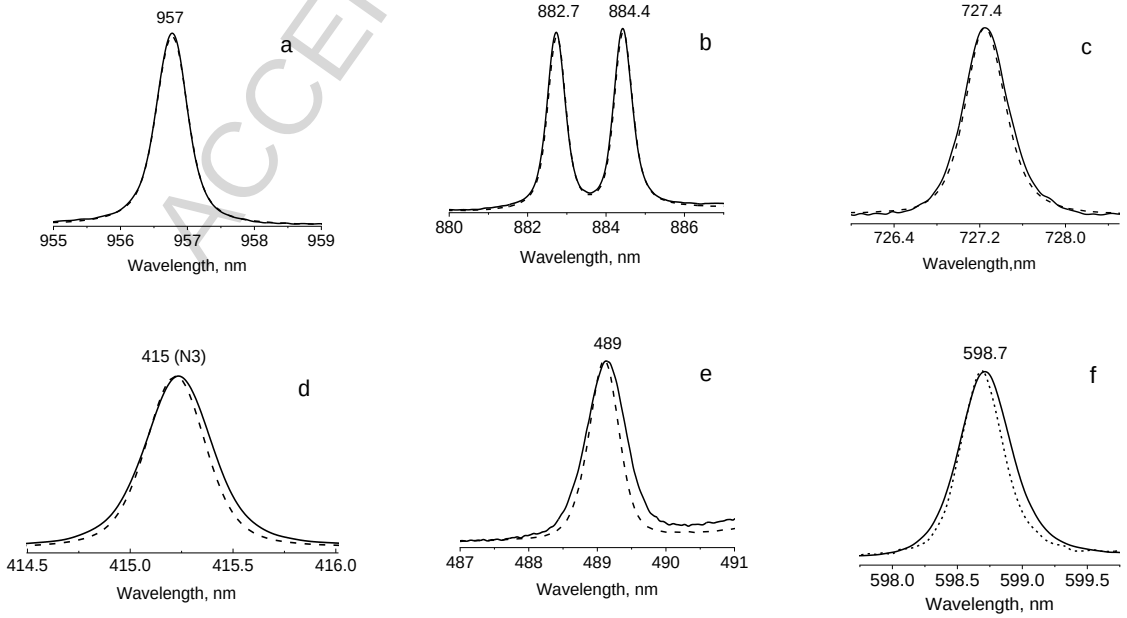

Fig. 7. PL spectra of ZPLs of some centers, ZPLs which show no measurable broadening (a-c), and centers, which show minor ZPL broadening (d-f) after LPHT annealing. Spectra of LPHT-annealed samples are shown with solid lines. Spectra of HPHT-annealed samples are shown with dashed lines. Peak intensities of lines on each graph are adjusted to equal magnitude for clarity.

While ZPLs of some optical centers might broaden considerably, there was no obvious broadening of Raman line (Fig. 8).

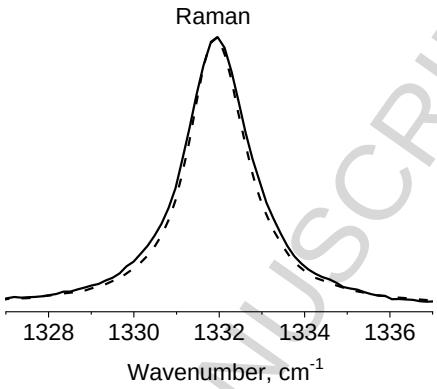

Fig. 8. Spectra of Raman line measure at room temperature in LPHT-annealed sample (solid line) and HPHT-annealed sample (dashed line). Peak intensities of the lines are adjusted to equal magnitude.

Measurements of the Raman line width in several places of cubic and octahedral sectors of as-grown as well as annealed samples revealed that in octahedral sector the line seemed to be broader on average by about 0.07 cm^{-1} in LPHT-annealed sample than in HPHT-annealed one. In cubic sector, this broadening was not more than 0.04 cm^{-1}. These values were comparable with the variations in the line width in as-grown samples and therefore were caused most probably by the variations in nitrogen content [53]. Thus, we believe that both LPHT annealing and HPHT annealing did not produce nonhomogeneous distortions of lattice all over the crystal. However, the strong broadening of some ZPLs is indicative of nonhomogeneous lattice distortions around corresponding defects. Based on the values of piezospectroscopic coefficients of centers NV^-, NV^0 and H3 [46, 55-57], we can deduce that the rate of non-homogeneous broadening of their ZPLs due to random stress is about 10, 9 and 16 meV/GPa, respectively. Thus, the experimentally observed broadening of ZPLs of 1.0 meV for NV^- center, 0.6 meV for NV^0 center and 1.2 meV for H3 center requires random stress at a level of 0.07 to 0.1 GPa. A long-range stress of this magnitude would result in a broadening of Raman line by 0.2 cm^{-1} [32, 46], what would be easily measured. Thus, the broadening of some ZPLs and the absence of broadening of Raman line suggest that the lattice distortions affecting some optical centers in LPHT-annealed diamond do not form all over the crystal but only in the proximity of these defects. Since the broadened ZPLs remain essentially symmetric and no spectral shift is observed, we assume that the local lattice distortions around defects are random.

The existence of two types of optical centers with high and low sensitivity of their ZPLs to LPHT annealing can be explained in two ways. First, the lattice distortions do not form around all defects. Second, there are defects with "rigid" and "soft" atomic structure [46, 58]. The "rigid" defects have

compact atomic structure, they are more stable than the surrounding crystal and therefore they do not feel the lattice distortions. The "soft" defects have diffused atomic structures which are more responsive to distortions of surrounding lattice. We believe that the "softness" of optical centers is the result of the presence of vacancies in the atomic structure. Absence of vacancies and presence of interstitials make optical center "rigid". Based on these considerations we can assume that the "rigid" metal-related centers do not contain vacancies, while most of nitrogen-related centers owe their "softness" to the vacancies in their atomic structure.

The results presented above suggest that LPHT annealing stimulates formation of local lattice distortions around native defects. We can offer two tentative explanations of this effect. The one is the formation of sp^2 bonded carbon (precursors of graphitization). These sp^2-bonded defects are not optically active in luminescence but create substantial lattice strain since sp^2-coordinated carbon (graphite) has much lesser atomic density than sp^3-coordinated carbon (diamond). The defects, even point defects, are structurally "weak" sites in crystal lattice and as such are triggers of graphitization at high temperatures. The enhanced graphitization around macroscopic defects like cracks and inclusions is a well-known effect of LPHT annealing. Here we speculate that the thermally-induced graphitization can be initiated by any lattice imperfections including point defects. Another explanation could be the diffusion of hydrogen and accumulation of hydrogen atoms around point defects. This is a very bold and speculative assumption for it implies considerable long-range diffusion of hydrogen into diamond to depths of tens of microns. However, we dare to assume this possibility considering our preliminary experiments on the influence of hydrogen atmosphere on the properties of optical centers in LPHT-annealed diamond (to be published). The results of these experiments reveal that the formation of optical centers and their spectroscopic parameters do depend on the presence of hydrogen during annealing at very high temperatures.

The lattice distortion around point defects reported in this communication is probably an explanation of broader ZPLs of NV centers seen after commercial HPHT annealing of natural diamonds [59]. Since commercial HPHT treatment is usually performed at pressures below the level of thermodynamic stability of diamond [8] the beginning of destruction of crystal lattice around point defects can occur in this case too. The enhanced susceptibility of diamond lattice to damage near point defects is not something entirely new. For instance, preferential production of vacancies near nitrogen defects during electron irradiation is a well-known effect [60, 61].

Conclusions

The presented results suggest that the behavior of major nitrogen- and metal-related defects in synthetic diamond during annealing at temperatures below 1900 °C does not depend significantly on pressure. The major difference between HPHT and LPHT annealing is the quality of the process in terms of structural integrity of the annealed diamonds and their graphitization. While it is generally believed that the bulk graphitization during LPHT annealing occurs primarily at macroscopic defects like cracks and inclusions, in this communication we put forward an idea that point defects may also be triggers of the thermally-induced damage of diamond crystal lattice at microscopic level. In case of optically active point defects, this lattice damage can be detected as broadening of ZPLs of their electron-phonon spectra. We also assume that one of the possible mechanisms of the ZPL broadening observed after LPHT annealing performed in hydrogen could be diffusion of hydrogen atoms and their accumulation around points defects.

A novel effect of LPHT annealing is the enhancement of luminescence efficiency. For now, we do not have a reasonable explanation of this effect. Two empirical explanations could be the higher concentration of optical centers produced during LPHT annealing, and the suppression of channels

of non-radiative recombination. Coexistence of the effect of the luminescence enhancement and the effect of the perturbation of optically active defects is in a seeming contradiction. Indeed, usually, luminescence intensity in solids is expected to be higher in perfect crystal lattice. However, in LPHT-annealed synthetic diamond it appears to be opposite. Although the mechanism of this luminescence enhancement is not understood yet, it could be of importance for some practical applications, like production of diamond micro- and nanoparticles used as fluorescence markers [62].

Qualitatively, HPHT annealing and LPHT annealing result in creation of the same nitrogen- and metal-related defects. However, quantitively relative concentrations of these defects may differ substantially. We assume that this difference is a result of higher concentration of structural defects induced by LPHT annealing.

Acknowledgements

Samples for this research and HPHT annealing were provided by company AdamasInvest, Minsk, Belarus.

This work was supported in part by the Belarusian National Research Programs "Functional and composite materials, nanomaterials".

References

[1] I. Kiflawi, H. Kanda, D. Fisher, S. C. Lawson, The aggregation of nitrogen and the formation of A centres in diamonds, Diamond and related materials, 6 (1997) 1643-1649.

[2] V.S. Vavilov, The possibilities and limitations of ion implantation into diamonds as compared to other doping techniques, Uspekhi Fizicheskikh Nauk, 164(4) (1994) 429-433 (in Russian).

[3] A.T. Collins, I. Kiflawi, The annealing of radiation damage in type Ia diamond. Journal of Physics: Condensed Matter, 21 (2009) 364209.

[4] J.W. Steeds, S. Kohn, Annealing of electron radiation damage in a wide range of Ib and IIa diamond samples. Diamond and Related Materials, 50 (2014) 110-122.

[5] M. Seal, The effect of surface orientation on the graphitization of diamond, Physica Status Solidi (b) 3 (1963) 658-664.

[6] V.R. Howes, The graphitization of diamond. Proceedings of the Physical Society, 80 (1962) 648-662.

[7] G. Davies, T. Evans, Graphitization of Diamond at Zero Pressure and at a High Pressure, Proceedings of the Royal Society of London. Series A, Mathematical and Physical Sciences, 328 (1972) 413-427.

[8] I.A. Dobrinets, V.G. Vins, A.M. Zaitsev, HPHT-Treated Diamonds: Diamonds Forever (Vol. 181), Springer Science & Business Media, 2013, pp. 257.

[9] G. Davies, The optical properties of diamond. Chemistry and physics of carbon, 13 (1977) 1-144.

[10] N.M. Kazuchits, M.S. Rusetsky, V.N. Kazuchits, A.M. Zaitsev, Aggregation of nitrogen in synthetic diamonds annealed at high temperature without stabilizing pressure, Diamond and Related Materials, 64 (2016) 202–207.

[11] V. G. Vins, A. P. Yelisseyev, S. S. Lobanov, A. Ye. Blinkov, APHT treatment of brown type Ia natural diamonds: Dislocation movement or vacancy cluster destruction?, Diamond and Related Materials, 19 (2010) 829-832.

[12] Chih-shiue Yan, Yogesh K. Vohra, Ho-kwang Mao, R. J. Hemley, Very high growth rate chemical vapor deposition of single-crystal diamond, PNAS 99 (2002) 12523-12525.

[13] Qi Liang, Chih-shiue Yan, Yufei Meng, Joseph Lai, S. Krasnicki, Ho-kwang Mao, R. J. Hemley, Enhancing the mechanical properties of single-crystal CVD diamond, Journal of Physics: Condensed Matter, 21 (2009) 364215.

[14] K. S. Moe, U. D'Haenens-Johansson, W. Wang, LPHT-Annealed Pink CVD Synthetic Diamonds, Gems & Gemology, Lab Notes, 51 (2) (2015).

[15] S. Eaton-Magaña, T. Ardon, A. M. Zaitsev, LPHT annealing of brown-to-yellow type Ia diamonds, Diamond and Related Materials, 77 (2017) 159-170.

[16] Yu-fei Meng, Chih-shiue Yan, Joseph Lai, S. Krasnicki, Haiyun Shu, Th. Yu, Qi Liang, Ho-kwang Mao, R. J. Hemley, Enhanced optical properties of chemical vapor deposited single crystal diamond by low-pressure/high-temperature annealing, PNAS, 105(46) (2008) 17620-17625.

[17] A. M. Zaitsev, On the way to mass-scale production of perfect bulk diamonds, PNAS 105(46) (2008) 17591–17592

[18] P. Hess, The mechanical properties of various chemical vapor deposition diamond structures compared to the ideal single crystal, Journal of Applied Physics, 111 (2012) 051101.

[19] Qi Liang, Chih-shiue Yan, Joseph Lai, Yu-fei Meng, S. Krasnicki, Haiyun Shu, Ho-kwang Mao, and R. J. Hemley, Large Area Single-Crystal Diamond Synthesis by 915 MHz Microwave Plasma-Assisted Chemical Vapor Deposition, Crystal Growth and Design, 14 (2014) 3234−3238.

[20] W. Wang, U. F. D'Haenens-Johansson, P. Johnson, K. S. Moe, E. Emerson, M. E. Newton, T. M. Moses, CVD Synthetic Diamonds from Gemesis Corp. Gems & Gemology, 48 (2012) 80-97.

[21] http://adamas.by

[22] N.M. Kazyuchits, A.V. Konovalova, I.I. Azarko, F.F. Yakotsuk, I.N. Bogdanov, Yu.K. Kabak, Effect of synthesis conditions on the impurity composition of STM Almazot diamond single crystals, Inorg. Mater. 50 (2) (2014) 130–135

[23] J.R. Kim, D.K. Kim, H. Zhu, R. Abbaschian, High pressure and high temperature annealing on nitrogen aggregation in lab-grown diamonds, Journal of materials science, 46 (2011) 6264-6272.

[24] http://www.freudlabs.com/high_t_equipment

[25] N.M. Kazuchits, M.S. Rusetsky, V.N. Kazuchits, A.M. Zaitsev, Cathodoluminescence of synthetic diamonds annealed at high temperature without stabilizing pressure, Diamond and Related Materials, 74 (2017) 41-44.

[26] N.M. Kazuchits, M.S. Rusetsky, J.I. Latushko, V.N. Kazuchits, A.M. Zaitsev, Nitrogen aggregation in synthetic Ib diamonds at high temperature without stabilizing pressure, Proceedings of the 11th International Conference "Interaction of radiation with solids", 23-25 September, 2015, Minsk, Belarus, p. 411-413 (in Russian).

[27] G.B. Bokii, G.N. Bezrukov, Ju.A. Kluev, A.M. Naletov, V.I. Nepsha, Natural and Synthetic Diamonds, Nauka, Moscow, (1986) (in Russian).

[28] I. Kiflawi, A.E. Mayer, P.M. Spear, J.A. Van Wyk, G.S. Woods, Infrared absorption by the single nitrogen and A defect centers in diamond, Philos. Mag. B, 69 (1994) 1141–1147.

[29] S.R. Boyd, I. Kiflawi, G.S. Woods, The relationship between infrared absorption and the A defect concentration in diamond, Philos. Mag. B, 69 (1994) 1149–1153.

[30] S.C. Lawson, D. Fisher, D.C. Hunt, M.E. Newton, On the existence of positively charged single-substitutional nitrogen in diamond, J. Phys. Condens. Matter, 10 (1998) 6171–6180.

[31] A. M. Zaitsev, K. S. Moe, W. Wang, Optical centers and their depth distribution in electron irradiated CVD diamond, Diamond and Related Materials, 71 (2016) 38-52.

[32] S. Prawer, R.J. Nemanich, Raman spectroscopy of diamond and doped diamond, Phil. Trans. R. Soc. Lond. A 362 (2004) 2537–2565.

[33] J. Walker, Optical absorption and luminescence in diamond, Reports on Progress in Physics, 42 (1979) 1605-1627.

[34] G. Davies, Properties and Growth of Diamond. INSPEC, London, UK, 1994.

[35] H. Kanda, K. Watanabe, Distribution of nickel related luminescence centers in HPHT diamond, Diamond and Related Materials 8 (1999) 1463-1469.

[36] A. Yelisseyev, Y. Babich, V. Nadolinny, D. Fisher, B. Feigelson, Spectroscopic study of HPHT synthetic diamonds, as grown at 1500 °C, Diamond and Related Materials, 11 (2002) 22-37.

[37] A.P. Yelisseyev, J.W. Steeds, Y.V. Babich, B.N. Feigelson, A new approach to investigation of nickel defect transformation in the HPHT synthetic diamonds using local optical spectroscopy, Diamond and Related Materials, 15 (2006) 1886-1890.

[38] I. Kiflawi, H. Kanda, S.C. Lawson, The effect of the growth rate on the concentration of nitrogen and transition metal impurities in HPHT synthetic diamonds, Diamond and Related Materials, 11 (2002) 204-211.

[39] Yu.V. Babich, B.N. Feigelson, Distribution of N+ centers in synthetic diamond single crystals, Inorg. Mater. 45 (2009) 616–619.

[40] S.P. Plotnikova, Classification and selection of natural diamonds for electronic applications, in: Almaz v elektronnoj tehnike (collection of articles), Moscow, Energoatomizdat, (1990) 156-170 (in Russian).

[41] F. De Weerdt, A. T. Collins, HPHT annealing of natural diamond. New Diam. Front. Carbon Technol, 17 (2007) 91-103.

[42] A. Yelisseyev, V. Nadolinny, B. Feigelson, S. Terentyev, S. Nosukhin, Spatial distribution of impurity defects in synthetic diamonds obtained by the BARS technology, Diamond and Related Materials, 5 (1996) 1113-1117.

[43] V.D. Antsygin, V.A. Gusev, A.A. Kalinin, I.N. Kuprianov, Yu.N. Paljanov, G.M. Rylov Some aspects of the transformation of defects in a synthetic diamond under high temperatures and pressures, Autometrya 1 (1998) 10–17 (in Russian).

[44] A.P. Yelisseyev, H. Kanda, Optical centers related to 3d transition metals in diamond, New Diamond Front. Carbon Technol. 17 (2007) 127–178.

[45] A.P. Yelisseyev, Optically Active Nickel Centers in Diamond: Spectroscopy, Structure, Transformation, Spatial distribution, 2009 (Dr. Sc. Thesis, Ekatirenburgin, Russian).

[46] A.M. Zaitsev, Optical Properties of Diamonds: A Data Handbook, Springer, Berlin, 2001.

[47] D. Fisher, S.C. Lawson, The effect of nickel and cobalt on the aggregation of nitrogen in diamond. Diamond and Related Materials, 7 (1998) 299-304.

[48] V.A. Nadolinny, A.P. Yelisseyev, J.M. Baker, D.J. Twitchen, M.E. Newton, B.N. Feigelson, O.P. Yuryeva, "Mechanisms of nitrogen aggregation in nickel- and cobalt-containing synthetic diamonds ", Diamond and Related Materials 9 (2000) 883–886.

[49] S.C. Lawson, H. Kanda, Nickel in diamond: an annealing study, Diamond and Related Materials, 2 (1993) 130–135.

[50] E. Pereira, L. Santos, Dynamics of S3 luminescence in diamond, J. Luminescence, 45 (1990) 454–457.

[51] V.A. Nadolinny, A.P. Yelisseyev, New paramagnetic centres containing nickel ions in diamond, Diamond and Related Materials, 3 (1993) 17–21.

[52] A.P. Yelisseyev, V. Nadolinny, HPHT annealing of synthetic diamonds as a promising method to control their properties and quality, in: M. Yoshikava, M. Murakawa, Y. Tzeng, W.A. Yarbrough (Eds.), Proc. 2nd Int. Conf. Appl. of Diamond Films and Related Materials, MYU, Tokyo 1993, p. 623.

[53] V.A. Nadolinny, A.P. Yelisseyev, J.M. Baker, M.E. Newton, D.J. Twitchen, S.C. Lawson, O.P. Yuryeva, B.N. Feigelson, A study of 13C hyperfine structure in the EPR of nickel nitrogen-containing centers in diamond and correlation with their optical properties, J. Phys.: Condens. Matter, 11 (1999) 7357–7376.

[54] N.V. Surovtsev, I.N. Kupriyanov, V.K. Malinovsky, V.A. Gusev and Yu.N. Pal'yanov, Effect of nitrogen impurities on the Raman line width in diamonds. J. Phys.: Condens. Matter 11 (1999) 4767–4774.

[55] G. Davies, M.F. Hamer, Optical Studies of the 1.945 eV Vibronic Band in Diamond, Proceedings of the Royal Society of London. Series A, Mathematical and Physical Sciences, 348 (1976) 285-298.

[56] G. Davies, M.H. Nazaré, M.F. Hamer, The H3 (2.463 eV) Vibronic Band in Diamond: Uniaxial Stress Effects and the Breakdown of Mirror Symmetry, Proceedings of the Royal Society of London. Series A, 351 (1976) 245-265.

[57] K. Mohammed, G. Davies, A.T. Collins, Uniaxial stress splitting of photoluminescence transitions at optical centres in cubic crystals: theory and application to diamond, J. Phys. C: Solid State Phys., 15 (1982) 2779-2788.

[58] A.M. Zaitsev, A.A. Melnikov, A.V. Denisenko, V.S. Varichenko, R. Job, W.R. Fahrner, Luminescence characterization and application of diamond, Mat. Res. Soc. Symp. Proc., 416 (1996) 113-124.

[59] W. Wang, R.Lu, T. Moses, "Photoluminescence Features of Carbonado Diamonds", News from Research, July 21 (2009), http://www.gia.edu/research-resources/news-from-research.

[60] G. Davies, B. Campbell, A. Mainwood, M. Newton, M. Watkins, H. Kanda, and T.R. Anthony Interstitials, Vacancies and Impurities in Diamond phys. stat. sol. (a), 186 (2001) 187–198.

[61] G. Davies, S.C. Lawson, A.T. Collins, A. Mainwood, and S.J. Sharp, Vacancy-related centers in diamond, Physical Review B, 46 (1992) 13157-13170.

[62] L. Dei Cas, S. Zeldin, N. Nunn, M. Torelli, O. Shenderova, A. M. Zaitsev, From Fancy Blue to Red: Controlled Production of a Vibrant Color Spectrum of Fluorescent Diamond Particles, to be published.

Graphical Abstract

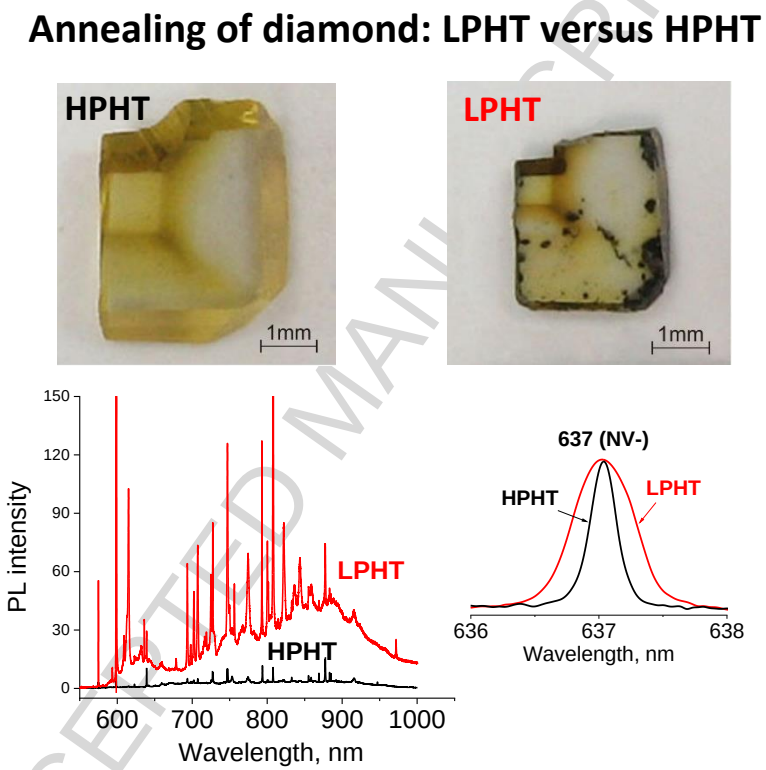

Highlights

Transformations of major nitrogen- and nickel-related defects in synthetic HPHT-grown diamond during annealing at temperatures below 1900°C does not depend on pressure.

Annealing without stabilizing pressure may considerably stimulate luminescence of HPHT-grown synthetic diamond.

In HPHT-grown synthetic diamonds, annealing without stabilizing pressure causes lattice distortions around point defects.

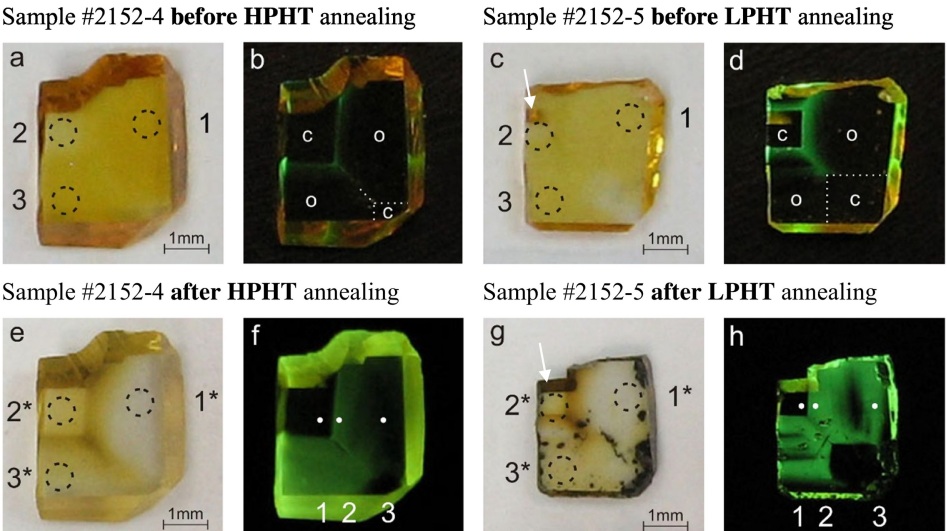
Sample #2152-4 **before HPHT** annealing
Sample #2152-5 **before LPHT** annealing
a
b
c
d
2
1
3
1mm
c
o
o
c
Sample #2152-4 **after HPHT** annealing
Sample #2152-5 **after LPHT** annealing
e
f
g
h
2*
1*
3*
1 2 3

Figure 1

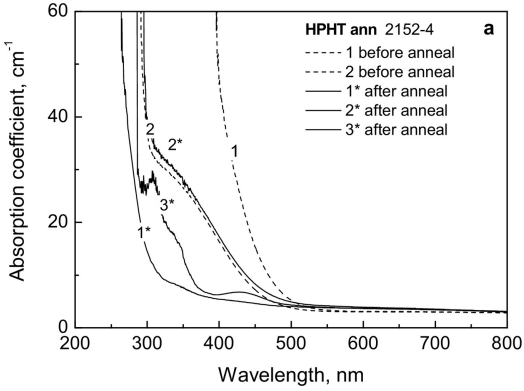
HPHT ann 2152-4
a
1 before anneal
2 before anneal
1* after anneal
2* after anneal
3* after anneal
Absorption coefficient, cm-1
Wavelength, nm
1
2
2*
3*
1*
0
20
40
60
200
300
400
500
600
700
800

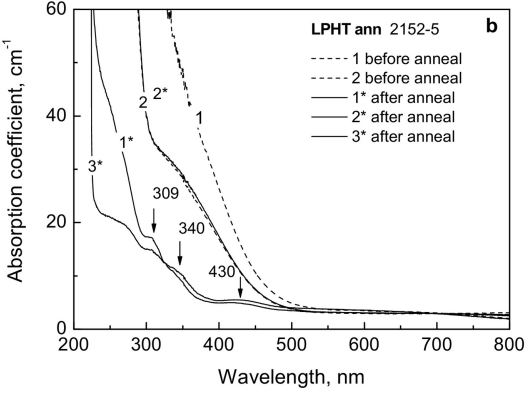
LPHT ann 2152-5
b
1 before anneal
2 before anneal
1* after anneal
2* after anneal
3* after anneal
Absorption coefficient, cm-1
Wavelength, nm
1
2
2*
3*
1*
309
340
430
0
20
40
60
200
300
400
500
600
700
800

Figure 2

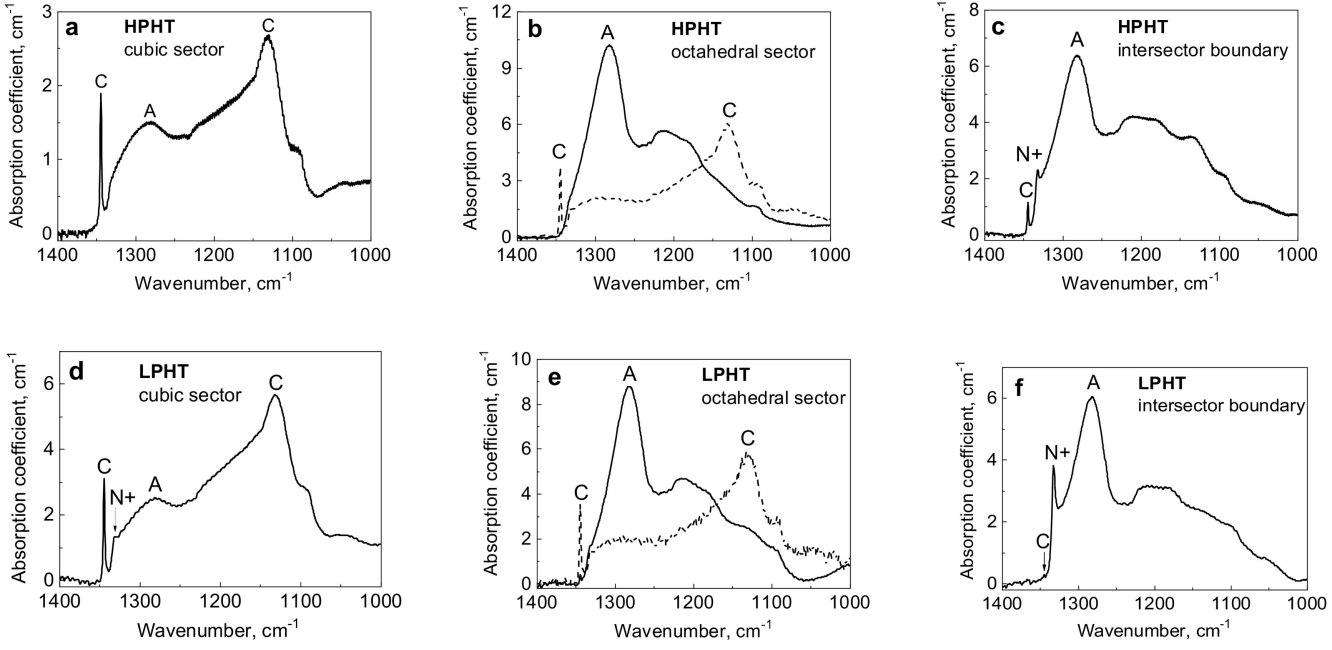
a
HPHT
cubic sector
b
HPHT
octahedral sector
c
HPHT
intersector boundary
d
LPHT
cubic sector
e
LPHT
octahedral sector
f
LPHT
intersector boundary
C
A
N+
Absorption coefficient, cm-1
Wavenumber, cm-1
1400
1300
1200
1100
1000

Figure 3

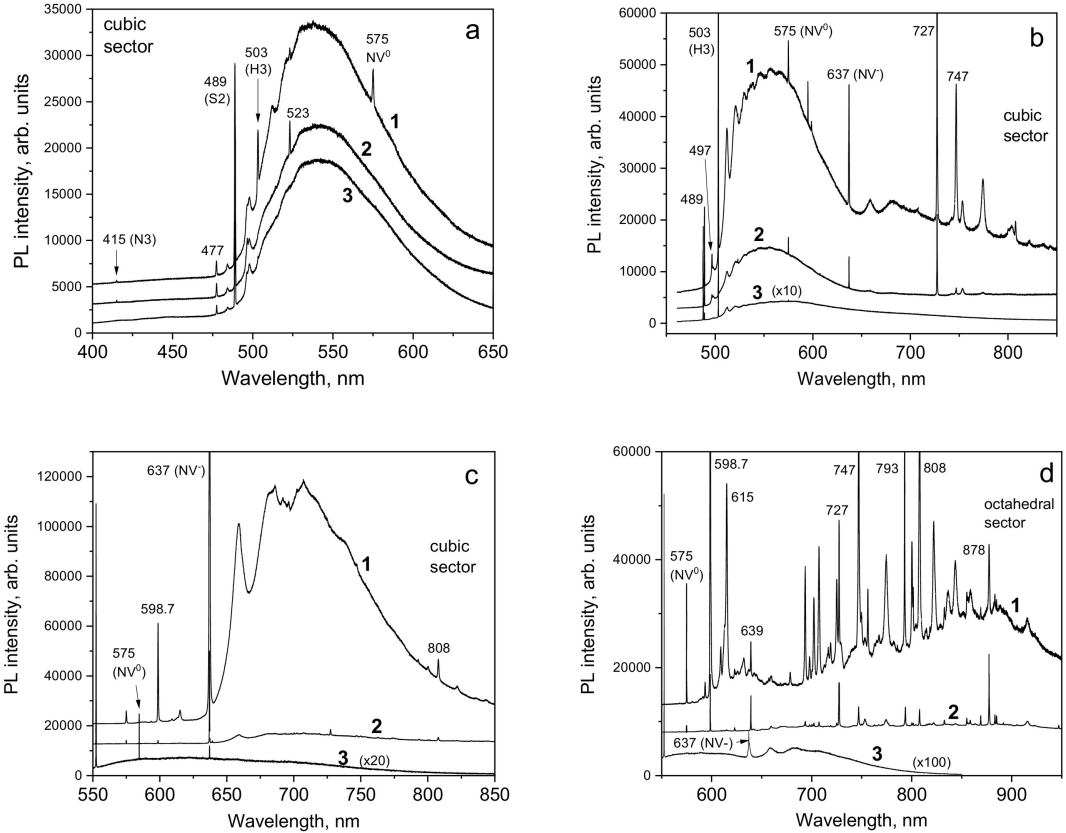
a
cubic sector
PL intensity, arb. units
Wavelength, nm
415 (N3)
477
489 (S2)
503 (H3)
523
575 NV0
1
2
3
b
503 (H3)
575 (NV0)
727
637 (NV-)
747
497
489
cubic sector
(x10)
c
637 (NV-)
598.7
575 (NV0)
808
cubic sector
(x20)
d
598.7
615
747
793
808
727
878
575 (NV0)
639
octahedral sector
637 (NV-)
(x100)

Figure 4

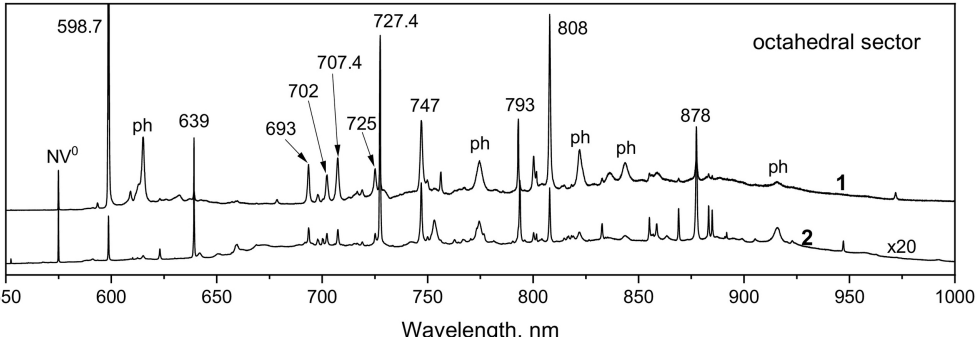
598.7
727.4
808
octahedral sector
707.4
702
693
639
725
747
793
878
NV0
ph
ph
ph
ph
ph
1
2
x20
550
600
650
700
750
800
850
900
950
1000
Wavelength, nm

Figure 5

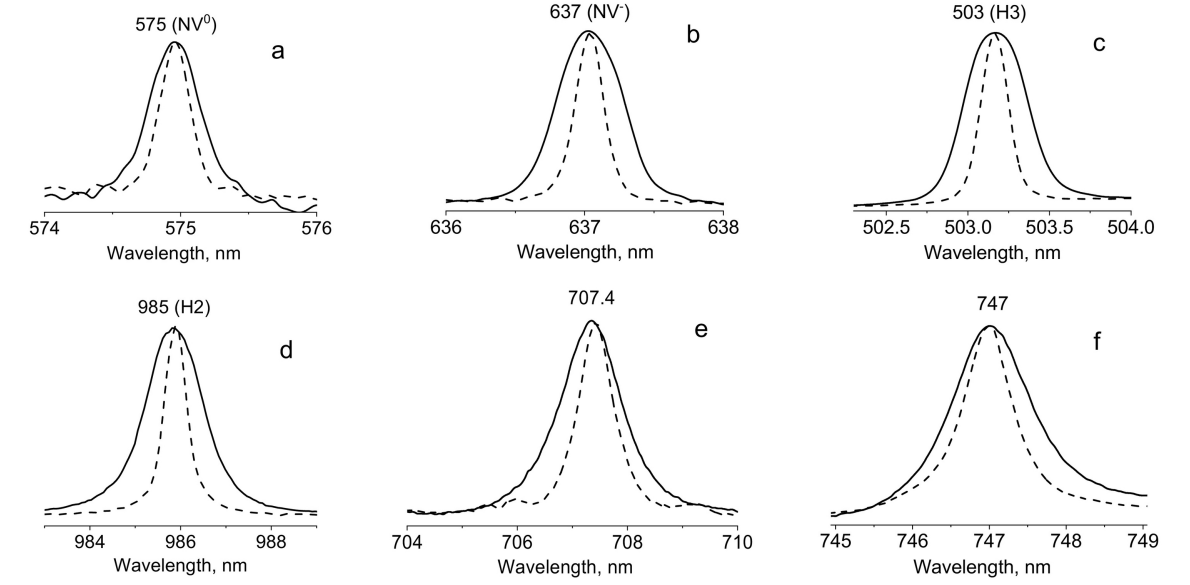
575 (NV0)
a
574
575
576
Wavelength, nm
637 (NV-)
b
636
637
638
Wavelength, nm
503 (H3)
c
502.5
503.0
503.5
504.0
Wavelength, nm
985 (H2)
d
984
986
988
Wavelength, nm
707.4
e
704
706
708
710
Wavelength, nm
747
f
745
746
747
748
749
Wavelength, nm

Figure 6

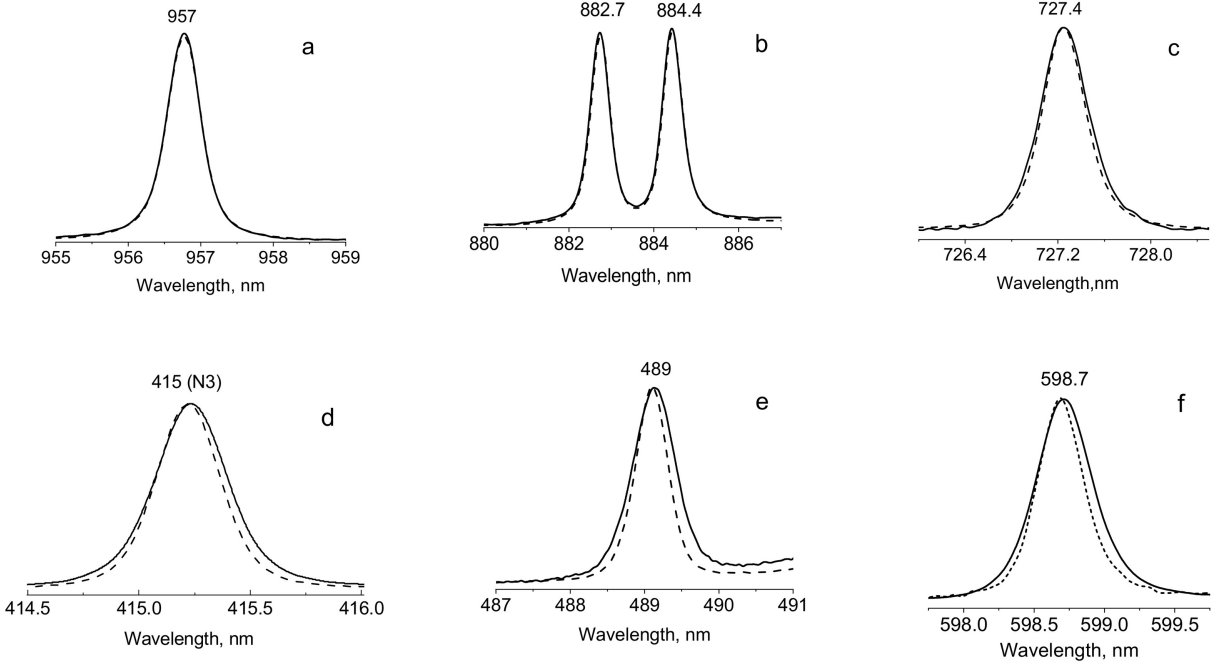
957
a
955
956
957
958
959
Wavelength, nm
882.7
884.4
b
880
882
884
886
Wavelength, nm
727.4
c
726.4
727.2
728.0
Wavelength,nm
415 (N3)
d
414.5
415.0
415.5
416.0
Wavelength, nm
489
e
487
488
489
490
491
Wavelength, nm
598.7
f
598.0
598.5
599.0
599.5
Wavelength, nm

Figure 7

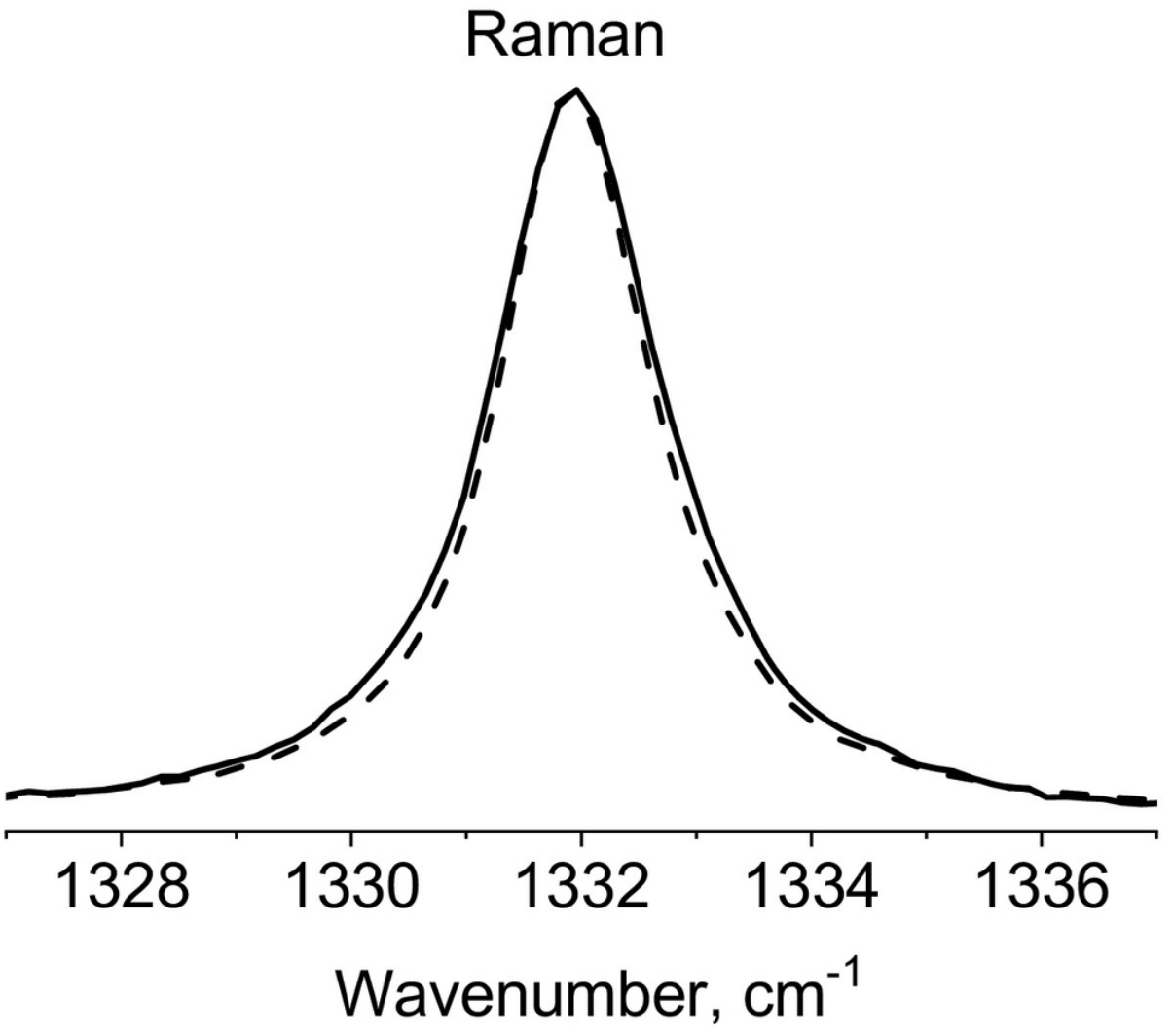

Figure 8